



**Melt Production Beneath Mt. Shasta from Boron
Data in Primitive Melt Inclusions**

Estelle F. Rose, *et al.*
Science **293**, 281 (2001);
DOI: 10.1126/science.1059663

***The following resources related to this article are available online at
www.sciencemag.org (this information is current as of July 10, 2008):***

Updated information and services, including high-resolution figures, can be found in the online version of this article at:

<http://www.sciencemag.org/cgi/content/full/293/5528/281>

This article **cites 10 articles**, 2 of which can be accessed for free:

<http://www.sciencemag.org/cgi/content/full/293/5528/281#otherarticles>

This article has been **cited by** 31 article(s) on the ISI Web of Science.

This article has been **cited by** 6 articles hosted by HighWire Press; see:

<http://www.sciencemag.org/cgi/content/full/293/5528/281#otherarticles>

This article appears in the following **subject collections**:

Geochemistry, Geophysics

http://www.sciencemag.org/cgi/collection/geochem_phys

Information about obtaining **reprints** of this article or about obtaining **permission to reproduce this article** in whole or in part can be found at:

<http://www.sciencemag.org/about/permissions.dtl>

Melt Production Beneath Mt. Shasta from Boron Data in Primitive Melt Inclusions

Estelle F. Rose,¹ *† Nobumichi Shimizu,¹ Graham D. Layne,¹ Timothy L. Grove²

Most arc magmas are thought to be generated by partial melting of the mantle wedge induced by infiltration of slab-derived fluids. However, partial melting of subducting oceanic crust has also been proposed to contribute to the melt generation process, especially when young and hot lithosphere is being subducted. The isotopic composition of boron measured in situ in olivine-hosted primitive melt inclusions in a basaltic andesite from Mt. Shasta, California, is characterized by large negative values that are also highly variable ($\delta^{11}\text{B} = -21.3$ to -0.9 per mil). The boron concentrations, from 0.7 to 1.6 parts per million, are lower than in most other arc lavas. The relation between concentration and isotopic composition of boron observed here supports a hypothesis that materials left after dehydration of the subducting slab may have contributed to the generation of basaltic andesite lavas at Mt. Shasta.

Boron is a geochemical tracer of recycling of crustal material into the mantle and of interaction of mantle-derived magma and crust. Boron isotope fractionation occurs during low-temperature and low-pressure processes, resulting in isotopic variations up to 90‰ among surface reservoirs (1). These reservoirs are enriched in boron (2) relative to the mantle (3), and interaction between mantle-derived melts and crustal reservoirs could alter the B isotopic composition of magmas. Subduction of the shallow reservoirs, such as sediments and/or altered oceanic crust (AOC), and subsequent release of fluid from them, could impart diverse isotopic signatures to the mantle wedge and thus to arc magmas.

Here, we determined the B isotopic compositions in individual melt inclusions hosted by high-Mg olivines in a primitive basaltic andesite from Mt. Shasta, California. The Cascadia system is characterized by subduction of young oceanic crust [age <6 million years (4)] and presents an end-member case where the possibility of a contribution from slab melting can be tested quantitatively. Melt inclusions hosted by high-Mg olivines are the least modified in a crustal magma chamber, and they represent the closest approach to melting and melt migration processes beneath Mt. Shasta.

The sample analyzed (sample 95-15) is a

basaltic andesite of the Misery Hill stage [80,000 to 10,000 years before the present (5)], collected from a cinder cone 10 km south of the summit. High-Mg olivines (forsterite content of 89.3 to 90.6) occur as phenocrysts in a partially crystalline ground mass (6). Melt inclusions are subspherical, 50 to 100 μm across, and partly crystalline. In addition to the growth of the host olivine, daughter crystals of clinopyroxene and occasional minor amphibole are observed. Degrees of post-entrapment crystallization range up to about 30% (20% olivine, 10% clinopyroxene) on the basis of residual glass composition. The B isotopic composition was determined with an ion microprobe (Cameca 1270), using techniques similar to earlier work (7, 8). The precision of $\delta^{11}\text{B}$ measurements (relative to National Bureau of Standards 951) is better than $\pm 1\%$ (1σ) for the synthetic silicate glass standard named GB 4 and on average $\pm 3\%$ for melt inclusion with B contents <1 ppm. Concentrations of B were determined with an ion microprobe (Cameca 3f), using an energy filtering-based procedure (9) and basaltic glass standards. The precision is assessed on the basis of counting statistics and ranges from 2 to 5% (1σ).

We obtained the following results: (i) The B concentrations, 0.67 to 1.64 ppm (Table 1), are much lower than in any other arc rocks reported thus far (Fig. 1A). Considering the degrees of post-entrapment crystallization, B concentrations in the initial melts could be even lower, by $\sim 40\%$. (ii) The $\delta^{11}\text{B}$ is highly variable, ranging from -21.3 to -0.9% . These melts must have been derived from sources of distinct $\delta^{11}\text{B}$ compositions. (iii) Three of seven melt inclusions analyzed have $\delta^{11}\text{B} < -10\%$. These large negative values are unusual for subduction zone magmas. Our results differ from the findings for other

arc magmas (10–13), reflecting the unique character of the Cascadia system.

The B concentrations measured in the melt inclusions are similar to those in mid-ocean ridge basalts [MORB (12)]. This result indicates that the source rocks for these melts, relative to depleted MORB mantle [DMM (14)], are at least as depleted in B. This observation is not consistent with a hypothesis of fluid-induced melting of the mantle wedge, because B is considered to be partitioned into the fluid (14), and, relative to DMM, fluid-infiltrated mantle should be enriched in B. For instance, a fluid released from an altered basalt (10 ppm B) could contain 500 ppm B with a fluid/rock partition coefficient of 50. This fluid would increase the mantle wedge B concentration to 1.5 ppm, even when only 0.03% of fluid is added (15). This B concentration is about a factor of 10 greater than that in DMM (16). Melting of the fluid-modified mantle wedge would produce melts with B concentrations higher than 1.5 ppm (assuming that B is perfectly incompatible, 10% melting would yield 15 ppm B in the melt). Direct melting of AOC (>10 ppm B) or sediments (~ 100 ppm B) would produce melts with even higher B contents, which is unrealistic for the origin of the Mt. Shasta melts. Two of the melt inclusions in our sample have $\delta^{11}\text{B}$ at -21.3 and -17.0% . These values are much lower than those for AOC ($+6\%$) and sediment ($> -15\%$), and, together with low B concentrations, argue against direct melting of these sources.

Dehydration of a subducting slab extracts B into the fluid and leaves residues that are depleted in B. Recent studies have shown that $\delta^{11}\text{B}$ of dehydration residues (prograde metamorphic rocks) become increasingly lighter with increasing degree of dehydration (17–20). Therefore, dehydration residues become in-

Table 1. B isotopic composition and concentration (ppm) in melt inclusions from sample 95-15. B isotopic compositions are expressed in per mil (‰) as $\{[(^{11}\text{B}/^{10}\text{B})_{\text{sample}} / (^{11}\text{B}/^{10}\text{B})_{\text{standard}}] - 1\} \times 1000$, where the standard is National Bureau of Standards 951 and $(^{11}\text{B}/^{10}\text{B})_{\text{standard}} = 4.04558$ (29). B concentrations were determined with a Cameca IMS 3f ion microprobe with an energy offset of -90 V using a working curve based on basalt glasses. Analytical uncertainties (in ppm) are based on counting errors.

Melt inclusion number	$\delta^{11}\text{B}$ (‰)	$\pm 1\sigma_{\text{mean}}$	B (ppm)	$\pm 1\sigma$
95-15-1-1	-10.1	0.8	1.64	0.03
95-15-1-5	-0.9	2.7	1.02	0.03
95-15-1-6	-7.3	1.3	0.67	0.02
95-15-1-7	-2.7	1.2	0.79	0.02
95-15-2-1	-21.3	2.5	1.48	0.03
95-15-2-3	-16.9	3.1	0.74	0.03
95-15-2-6	-2.5	6.6	0.78	0.02
95-15-2-9	-1.1	5.8	0.83	0.02

¹Department of Geology and Geophysics, Woods Hole Oceanographic Institution, Woods Hole, MA 02543, USA. ²Department of Earth, Atmosphere and Planetary Sciences, Massachusetts Institute of Technology, Cambridge, MA 02139, USA.

*Present address: Institute for Study of the Earth's Interior–PML, Okayama University at Misasa, Tottori-ken, 682-0193, Japan.

†To whom correspondence should be addressed. E-mail: erose@pheasant.misasa.okayama-u.ac.jp

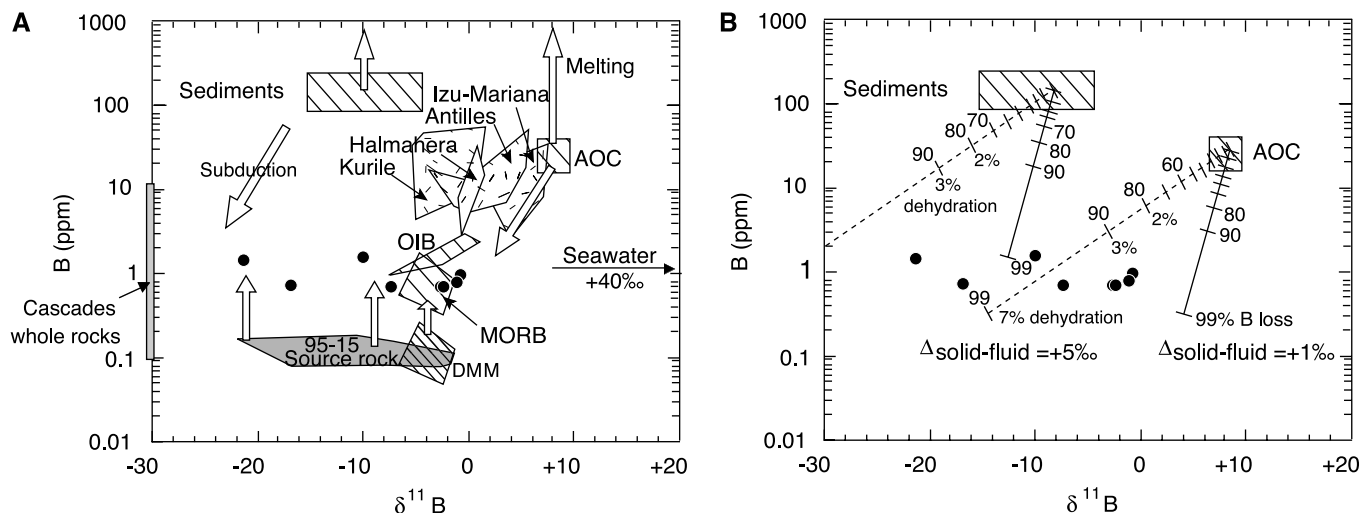


Fig. 1. (A) Isotopic composition and concentration of B in melt inclusions hosted by high-Mg olivines in basaltic andesite (95-15) from Mt. Shasta (solid circles). Striped areas are B reservoirs relevant to this study (12, 14, 27). The areas with confetti denote B characteristics of island arc rocks (whole rocks) in the literature (10, 11, 13, 26); the shaded vertical bar on the y axis represents Cascades whole rocks [B concentrations only (27)]. The dark-shaded area marked "source rock" is where the potential source rocks for 95-15 melt inclusions lie, and is derived from the present results by lowering the B contents by a factor of 10 (equivalent to 10% melting for a perfectly incompatible element) with $\delta^{11}\text{B}$ unchanged. Arrows indicate how B concentration and B isotopic composition characteristics vary in melting and subduction processes. **(B)** Diagram showing how major B reservoirs for

the subduction system (AOC and sediments) are reconciled with the observed B characteristics of the Shasta melt inclusions (solid circles). Solid and dashed lines originating from AOC and sediments are theoretical trajectories for subducting AOC and sediments. The trajectories were calculated using an open-system Rayleigh model by which B is efficiently extracted in fluid and isotopic fractionation occurs during dehydration. It was assumed that the partition coefficient K_d for B between solid phase (i.e., AOC or sediments) and fluid is 0.015 (21) and that the isotopic fractionation factor between fluid and solid Δ_{f-s} is +1‰ (solid curves) or +5‰ (dashed curves). Tick marks with large numbers denote amounts of boron (in weight percent) extracted from the system. Small numbers denote amounts of water (in weight percent) extracted from the system.

creasingly depleted in B, and isotopically they become increasingly lighter (larger negative $\delta^{11}\text{B}$). Exact pathways of B depletion and isotopic fractionation depend on the partitioning of B and the magnitude of isotopic fractionation between fluid and rock (14, 21); these variables are not well known for natural conditions, nor are they considered to be constant during polybaric and polythermal dehydration processes. The isotopic fractionation is also influenced by the pH of the fluid (14, 21). Assuming that the partition coefficient of B between solid and fluid $K_d = 0.015$ (21), and assuming that the B isotopic fractionation factor between fluid and solid Δ_{f-s} ($= \delta^{11}\text{B}_{\text{fluid}} - \delta^{11}\text{B}_{\text{solid}}$) = +1 or +5‰, an open-system Rayleigh model yields B trajectories from AOC and sediment (Fig. 1B). Instantaneous fluid compositions track the solid residue trajectories with greater B concentration (by a factor of 67) and with heavier isotopic composition (by +1 or +5‰). If fluid fractions released during dehydration are "pooled" together, mass balance would dictate that the pooled fluid would be indistinguishable from the starting material. The B concentrations and B isotopic compositions shown as "95-15 source rock" (Fig. 1) are derived from the melt inclusion data by lowering the B content by a factor of 10 (equivalent to 10% melting for a perfectly incompatible element) with $\delta^{11}\text{B}$ unchanged. This range is reached from AOC and sediment sources after removal of more than 99% of the B. Extraction of B from the system is much more efficient than removal of water because of low K_d . With $K_d = 0.015$, the

system loses only 7% of original water when more than 99% of B is removed; with $K_d = 0.05$, a 30% water loss occurs when 99.6% of B is removed.

Although exact pathways are uncertain, the dehydration process results in increasingly lower B concentration and increasingly light B isotopic composition in both residual rock and instantaneous fluid. Therefore, the B characteristics observed here suggest that the primitive melt inclusions contain components derived from (i) melting of dehydrated residues (i.e., a subducted slab) and/or (ii) melting of the mantle wedge triggered by infiltration of a late-stage B-poor fluid. The B systematics alone are not sufficient to choose between the two possibilities. Trace element signatures such as a high Sr/Y [up to 200 (22)] and covariation of Ti/Zr and La/Sm have been proposed to indicate the role of slab melting (10, 22, 23). However, the major element composition of the primitive basaltic andesite bears little resemblance to a siliceous slab melt and indicates a noticeable contribution from melting of depleted mantle peridotite source. High pre-eruptive H_2O contents (6, 12) postulated for Mt. Shasta lavas are unlike those of hypothesized slab melts (22, 23) that are viewed as products of volatile-free melting of subducted oceanic crust. Therefore, the slab component in the Mt. Shasta primitive basaltic andesite may be hydrous fluid released after extensive B removal or H_2O -rich slab melt derived from dehydration residues that has been reequilibrated with the overlying mantle wedge, preserving evidence for progressive dehydra-

tion of the slab source in its B characteristics. It is noteworthy that the B concentration and B isotopic composition characteristics observed here reflect dehydration and extensive extraction of B, which is expected for hot subduction of the Cascadia system (24, 25). On the other hand, for arc systems dominated by fluid-induced melting of the mantle wedge, the B characteristics of the melts would resemble those of major fluid reservoirs such as AOC or sediments. The literature data for the Halmahera (10), Izu-Bonin (11), Antilles (26), and Kurile (13) arc systems suggest that magmas were derived from the mantle wedge and AOC source (Fig. 1A). Variable $\delta^{11}\text{B}$ found in our melt inclusions reflects locally heterogeneous sources of B and could indicate a metamorphic complex containing metasedimentary and metabasaltic lithologies as sources for hydrous slab melts.

References and Notes

1. M. Palmer, *Geophys. Res. Lett.* **23**, 3479 (1996).
2. M. G. Truscott, D. M. Shaw, J. J. Cramer, *Bull. Geol. Soc. Finland* **58**, 169 (1986).
3. J. G. Ryan, C. H. Langmuir, *Geochim. Cosmochim. Acta* **57**, 1489 (1993).
4. R. D. Hyndman, T. J. Lewis, *Can. J. Earth Sci.* **32**, 1611 (1995).
5. R. L. Christiansen et al., *U.S. Geol. Surv. Open File Rep.* 0196-1497 (1977).
6. T. L. Grove, S. W. Parman, S. A. Bowring, R. C. Price, M. B. Baker, *Contrib. Mineral. Petrol.*, in press.
7. M. Chaussidon, F. Albarède, *Earth Planet. Sci. Lett.* **108**, 229 (1992).
8. M. Chaussidon, F. Robert, D. Mangin, P. Hanon, E. F. Rose, *Geostandard. Newsl.* **21**, 7 (1997).
9. N. Shimizu, S. R. Hart, *Annu. Rev. Earth Planet. Sci.* **10**, 483 (1982).

10. M. R. Palmer, *Geology* **19**, 215 (1991).
11. T. Ishikawa, E. Nakamura, *Nature* **370**, 205 (1994).
12. M. Chaussidon, A. Jambon, *Earth Planet. Sci. Lett.* **121**, 277 (1994).
13. T. Ishikawa, F. Tera, *Earth Planet. Sci. Lett.* **152**, 123 (1997).
14. M. Chaussidon, G. Libourel, *Geochim. Cosmochim. Acta* **57**, 5053 (1993).
15. E. Stolper, S. Newman, *Earth Planet. Sci. Lett.* **121**, 293 (1994).
16. M. Chaussidon, B. Marty, *Science* **269**, 383 (1995).
17. A. E. Moran, V. B. Sisson, W. P. Leeman, *Earth Planet. Sci. Lett.* **111**, 331 (1992).
18. G. E. Bebout, J. G. Ryan, W. P. Leeman, *Geochim. Cosmochim. Acta* **57**, 2227 (1993).
19. S. M. Peacock, R. L. Hervig, *Chem. Geol.* **160**, 281 (1999).
20. T. Nakano, E. Nakamura, *Phys. Earth Planet. Inter.*, in press.
21. C.-F. You, A. J. Spivack, J. M. Gieskes, J. B. Martin, M. L. Davison, *Mar. Geol.* **129**, 351 (1996).
22. N. Shimizu, T. L. Grove, *Abstract Volume of AGU Fall Meeting* (American Geophysical Union, Washington, DC, 1998).
23. M. J. Defant, M. S. Drummond, *Nature* **347**, 662 (1990).
24. W. P. Leeman, D. R. Hildreth, Z. Palacz, N. Rogers, *J. Geophys. Res.* **95**, 19561 (1990).
25. M. B. Baker, T. L. Grove, R. Price, *Contrib. Mineral. Petrol.* **118**, 111 (1994).
26. H. J. Smith, W. P. Leeman, J. Davidson, A. J. Spivack, *Earth Planet. Sci. Lett.* **146**, 303 (1997).
27. A. J. Spivack, J. M. Edmond, *Geochim. Cosmochim. Acta* **51**, 1033 (1987).
28. M. R. Palmer, A. J. Spivack, J. M. Edmond, *Geochim. Cosmochim. Acta* **51**, 2319 (1987).
29. We thank M. Chaussidon, P. B. Kelemen, and K. T. Koga for fruitful discussions, and the other regular Woods Hole geology and geophysics seminar participants for their constructive comments. Supported by Programme Lavoisier, France, and by a J. Steward Johnson scholarship from Woods Hole (E.F.R.).

7 February 2001; accepted 12 June 2001

Freshwater Forcing of Abrupt Climate Change During the Last Glaciation

Peter U. Clark,^{1*} Shawn J. Marshall,² Garry K. C. Clarke,³ Steven W. Hostetler,⁴ Joseph M. Licciardi,^{1†} James T. Teller⁵

Large millennial-scale fluctuations of the southern margin of the North American Laurentide Ice Sheet occurred during the last deglaciation, when the margin was located between about 43° and 49°N. Fluctuations of the ice margin triggered episodic increases in the flux of freshwater to the North Atlantic by rerouting continental runoff from the Mississippi River drainage to the Hudson or St. Lawrence Rivers. We found that periods of increased freshwater flow to the North Atlantic occurred at the same time as reductions in the formation of North Atlantic Deep Water, thus providing a mechanism for observed climate variability that may be generally characteristic of times of intermediate global ice volume.

A leading hypothesis about the origin of the large and abrupt fluctuations in high-latitude climate on millennial time scales invokes changes in the rate of formation of North Atlantic Deep Water (NADW) and their attendant effect on oceanic heat transport (1, 2). Numerous modeling studies demonstrate that the Atlantic thermohaline circulation (THC) is sensitive to the freshwater budget at the sites of deepwater formation (3–5): Increased freshwater flux to the North Atlantic decreases the formation of deep water, thereby reducing meridional heat transport, which causes cooling of the high latitudes. During glaciations, the circum-North Atlantic ice sheets would have been a ready source of fresh water, but in most cases

the causes of increased freshwater flux from these ice sheets to the North Atlantic and their exact relationship to abrupt climate change are unknown. The best-documented case of such freshwater forcing occurred during the Younger Dryas cold interval, when continental runoff that was rerouted from the Mississippi River to the St. Lawrence River at 11,000 ¹⁴C years before the present (yr B.P.) [13,000 calendar yr B.P. (cal yr B.P.)] reduced NADW formation (6–9). This mechanism for large-scale cooling has been regarded as unique to the Younger Dryas, however, and alternative mechanisms have been proposed to explain other millennial-scale climate fluctuations (10). Our new reconstructions of North American runoff (11, 12) suggest that the freshwater rerouting that caused the Younger Dryas was, in fact, one of a number of similar events that occurred when the southern margin of the Laurentide Ice Sheet (LIS) was located in the Great Lakes region (Fig. 1). Here, we compare our time series of North American runoff during the last deglaciation to high-resolution records of North Atlantic climate and conclude that these other rerouting events caused abrupt climate change in the North Atlantic region similar to that of the Younger Dryas.

Proxy records of climate and ocean circulation since the last glacial maximum (LGM)

indicate that initial warming in the North Atlantic region was accompanied by an increase in the rate of THC (Fig. 2). Assuming that the detrended record of atmospheric radiocarbon ($\Delta^{14}\text{C}$) is primarily a signal of ocean circulation (13), the post-LGM decrease in $\Delta^{14}\text{C}$ suggests that THC increased to essentially interglacial levels by 19,000 cal yr B.P. (19.0 cal kyr B.P.) (Fig. 2B). The Greenland oxygen isotope ($\delta^{18}\text{O}$ record), on the other hand, indicates that air temperatures remained relatively cold, which suggests that low atmospheric greenhouse gas concentrations and large ice sheets partially attenuated ocean-induced warming of the North Atlantic region. In addition, convection in the North Atlantic basin may have been restricted to intermediate depths, which allowed substantial sequestering of atmospheric ¹⁴C while contributing less heat than would have been released from deepwater formation (13).

Our reconstruction of rerouting events suggests that these initial deglacial warming trends were subsequently reversed by three sequential periods of increased freshwater flow to the North Atlantic originating from two rerouting events through the Hudson River (labeled R7 and R8 in Fig. 2F) that bracket increased iceberg discharge, culminating in Heinrich event 1 (Fig. 2E). During this Oldest Dryas cold event, proxies of ocean circulation identify a long-term decrease in the rate of THC that was episodically interrupted by large variations in the rate, depth, or location of deepwater formation (Fig. 2, B and C). The climate of the North Atlantic region remained cold during the Oldest Dryas (Fig. 2A), suggesting that despite apparent variability in deepwater formation, the net meridional heat transport into the North Atlantic basin remained reduced.

The abrupt warming of the Bølling at 12.8 ¹⁴C kyr B.P. (14.6 cal kyr B.P.) coincides with the end of the second rerouting event through the Hudson River (Fig. 2). Proxies of ocean circulation imply that THC also increased to interglacial levels similar to those preceding the Oldest Dryas (Fig. 2B). In contrast to pre-Oldest Dryas conditions, however, the invigorated THC at the start of the Bølling was accompanied by an increase in

¹Department of Geosciences, Oregon State University, Corvallis, OR 97331, USA. ²Department of Geography, University of Calgary, Calgary, Alberta T2N 1N4, Canada. ³Department of Earth and Ocean Sciences, University of British Columbia, Vancouver, British Columbia V6T 1Z4, Canada. ⁴U.S. Geological Survey, Department of Geosciences, Oregon State University, Corvallis, OR 97331, USA. ⁵Department of Geological Sciences, University of Manitoba, Winnipeg, Manitoba R3T 2N2, Canada.

*To whom correspondence should be addressed. E-mail: clarkp@ucs.orst.edu

†Present address: Department of Marine Chemistry and Geochemistry, Woods Hole Oceanographic Institution, Woods Hole, MA 02543, USA.